

## Chain-Length-Dependent Relaxation Scenarios in an Oligomeric Glass-Forming System: From Merged to Well-Separated $\alpha$ and $\beta$ Loss Peaks

J. Mattsson,<sup>1,\*</sup> R. Bergman,<sup>1</sup> P. Jacobsson,<sup>1</sup> and L. Börjesson<sup>2</sup>

<sup>1</sup>*Department of Experimental Physics, Chalmers University of Technology, SE-412 96 Göteborg, Sweden*

<sup>2</sup>*Department of Applied Physics, Chalmers University of Technology, SE-412 96 Göteborg, Sweden*

(Received 19 October 2002; published 21 February 2003)

We have studied the relaxation dynamics of a homologous series of propylene glycol based dimethyl ethers in the supercooled regime by means of broadband dielectric spectroscopy. The system is chosen in order to minimize changes of the intermolecular interactions with varying molecular weight,  $M$ . A gradual transformation from a scenario of well-separated to one of merged  $\alpha$  and  $\beta$  loss peaks was observed with decreasing  $M$ . The results give strong evidence for the currently debated excess wing being due to an underlying  $\beta$  relaxation. The study suggests that the main difference between glass formers with and without excess wings is the relaxation time at the merging temperature.

DOI: 10.1103/PhysRevLett.90.075702

PACS numbers: 64.70.Pf, 61.25.Em, 77.22.Gm

Understanding the liquid-glass transition and its related dynamics is one of the most important and challenging endeavors in condensed matter physics [1]. The glass transition related relaxation scenario encompasses the drastic viscous slowdown ( $\sim 15$  decades in relaxation time) of the supercooled liquid, which ultimately brings the liquid into the glassy state. A glass-forming liquid generally shows a non-Arrhenius temperature dependence of viscosity and the related  $\alpha$  relaxation time. In addition to the primary  $\alpha$  relaxation process a secondary, so-called Johari-Goldstein (J-G),  $\beta$  relaxation [2] often exists at high frequencies. In contrast to the  $\alpha$  relaxation, the  $\beta$  process normally follows an Arrhenius temperature dependence, i.e.,  $\ln(\tau_\beta) \propto 1/T$ . At high temperatures the primary and secondary relaxations merge and form one effective process [3].

In some supercooled liquids the  $\beta$  relaxation appears to be absent. Instead, in the dielectric loss  $\epsilon''$  an excess contribution to the high-frequency power law of the  $\alpha$  peak,  $\epsilon'' \propto f^{-\beta}$ , shows up a few decades above the  $\alpha$  peak frequency  $f_p$  [4]. This so-called excess wing has been found to be a common feature of glass-forming liquids without a well resolved  $\beta$  process. It can be well described by a second power law,  $\epsilon'' \propto f^{-\gamma}$ , with  $\gamma < \beta$  [4]. There is today no commonly accepted explanation for the microscopic origin of the excess wing, although some theoretical approaches have been proposed [3,5–7]. Often it is assumed that the excess wing and the  $\beta$  relaxation are different phenomena [8], and even the existence of two types of glass formers have been proposed: type *A* systems with an excess wing and type *B* systems with a  $\beta$  process [9]. In contrast, another picture has been suggested in which both the  $\beta$  process and the excess wing phenomena have the same or at least very similar physical origin [10–12]. The implication of this would be that  $\beta$  (as well as  $\alpha$ ) relaxations are fundamental features of the glass transition. Indeed, dielectric measurements extended to very low frequencies, while maintaining ther-

mal equilibrium, have shown that the excess wing, for low enough temperatures, shows up as a separate shoulder suggesting an underlying  $\beta$  peak [11]. Based on dielectric relaxation measurements at high pressures, arguments have been raised both in support of [13,14] and against [15] such a picture.

A way to test the hypothesis that the wing is due to an underlying  $\beta$  relaxation is to study a system where the separation between the  $\alpha$  and  $\beta$  processes can be tuned, while the nature of the relaxation processes stays unchanged. One possibility is to vary the chain length in a system for which the separation of the two main relaxations are a function of molecular weight, whereas the intermolecular interactions are expected to be the same. To our knowledge, only two chain-length studies have been performed with focus on the excess wing [16,17]. These studies, which were both performed on hydrogen bonded liquids, support the idea of the excess wing being caused by an underlying  $\beta$  process. However, for the investigated systems, the intermolecular interactions change substantially with chain length, thus rendering a conclusive analysis difficult.

In order to obtain information on the development of the excess wing without the disturbance from the hydrogen bonding properties we have chosen to study a homologous series of propylene glycol based dimethyl ethers,  $\text{CH}_3\text{O}-[\text{CH}_2\text{CH}(\text{CH}_3)\text{O}]_n-\text{CH}_3$ , including samples corresponding to  $n = 1, 2, 3$  and  $\approx 7$ . The monomer, dimer, and trimer can be regarded as monodisperse, while for the higher  $M$  sample  $n$  corresponds to the peak molecular weight. We have further included the hydroxyl capped polymer, polypropylene glycol, with  $M = 4000$  ( $n \approx 69$ ) as a good approximation of the polymeric behavior for the dimethyl ethers, since the influence of the end groups is marginal at such high  $M$  [18–20]. The samples will in the following be termed monomer, dimer, trimer, heptamer, and polymer, respectively.

The five samples were measured over a broad frequency ( $10^{-2}$ – $10^7$  Hz) and temperature range, using a high resolution dielectric spectrometer (Novocontrol Alpha). Asymmetric (Kohlrausch-Williams-Watts-type [21]) and symmetric (Cole-Cole [21]) response functions were fitted to the primary and secondary relaxation peaks, respectively. A detailed description of the experimental procedure and the subsequent analysis can be found in [20].

Figure 1 shows data taken at temperatures close to the glass transition  $T_g$  (here defined as the temperature where the relaxation time reaches 100 s) for all five samples of the study. The data have been scaled with the peak frequency and the peak amplitude in order to facilitate comparisons of the loss processes. It is clear that there is a large variation of the relative position and strength of the secondary processes. For the polymer and the heptamer, a relatively strong and distinct  $\beta$  peak is seen to be well separated from the  $\alpha$  peak, and also for the trimer the  $\beta$  peak is discernible. The inset to the right in Fig. 1 shows raw data for the heptamer, where both the  $\alpha$  and  $\beta$  relaxations are clearly observed over a large temperature and frequency range. The lower the molecular weight is, however, the smaller the relative distance between the two relaxations become. The  $\beta$  peak for the dimer is almost submerged under the much stronger  $\alpha$  loss peak, even though the  $\beta$  relaxation is clearly separated from the  $\alpha$  relaxation for temperatures below  $T_g$ . For the monomer

we observe only an excess contribution, at high frequencies, to the power law flank (dashed line) of the  $\alpha$  loss peak.

The behavior becomes even clearer in the derivative of the data, i.e.,  $d\log_{10}(\epsilon'')/d\log_{10}(f)$  vs  $\log_{10}(f)$  as shown in the inset to the left in Fig. 1. The secondary peak shifts systematically towards the  $\alpha$  peak with decreasing  $M$ . For the monomer, however, only a very weak feature is found at temperatures  $\sim T_g$ . The absolute strength of the  $\alpha$  process increases with decreasing  $M$  in the series, while that of the  $\beta$  process stays relatively unchanged [20]. Thus, for the lowest  $M$  samples the contribution from the secondary process is very weak compared to the primary one. The data within the box in the lower left inset of Fig. 1 shows  $d\log_{10}(\epsilon'')/d\log_{10}(f)$  vs  $\log_{10}(f)$  for the monomer at a temperature 11 K below  $T_g$ , where the decreased influence of the  $\alpha$  loss reveals that there is indeed a change from the high-frequency power law of the  $\alpha$  relaxation into a second power law, demonstrating the existence of an excess wing for the monomer. The rise of the derivative towards the highest frequencies, seen for all samples, is due to an additional fast relaxation process [20,22]. In agreement with these results we note that the analysis of the monomer  $\epsilon''(f)$  data at low temperatures requires the addition of a power law contribution with a negative exponent in the range 0.05–0.15, as expected for an excess wing contribution near  $T_g$  [23]. The decrease of the separation between the  $\alpha$  and  $\beta$  relaxations with decreasing  $M$  strongly suggests an identification of the observed excess wing with an underlying  $\beta$  relaxation.

We will in the following concentrate on results concerning the relaxation times (as calculated from the peak frequencies  $f_p$  by  $\tau = 1/2\pi f_p$ ) of the two processes. In Fig. 2, the obtained relaxation times for both the  $\alpha$  and  $\beta$  processes are plotted vs inverse temperature. A marked feature is the huge shift of the  $\alpha$  relaxation times and accordingly the glass transition temperature with molecular weight. The intuitively expected trend that higher  $M$  lead to slower relaxations is observed for both the  $\alpha$  and the  $\beta$  relaxations. We further note that the fragility [24] is very similar throughout the series, even though the samples span the range from monomer to polymer. This is in striking contrast to the behavior found in the corresponding hydrogen bonded glycol samples (propylene glycol, dipropylene glycol, etc.) [16,20], where the fragility shows strong variations with  $M$ . The  $\alpha$  relaxation time data can be well described by Vogel-Fulcher-Tammann (VFT) functions [3] over a large frequency range, as seen by the solid lines in Fig. 2. For the secondary process, in contrast, the data for all samples, except the monomer (where a  $\beta$  peak cannot be directly observed), are well described with an Arrhenius expression, as shown in Fig. 2.

We proceed by investigating the chain-length dependence of characteristic parameters describing the dynamics. Figure 3 shows results from such an investigation,

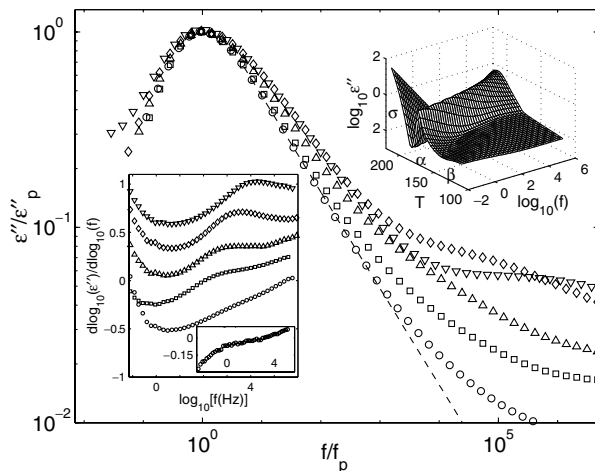


FIG. 1. Normalized dielectric loss for the monomer ( $\circ$ ), dimer ( $\square$ ), trimer ( $\triangle$ ), heptamer ( $\diamond$ ), and polymer ( $\nabla$ ) at temperatures corresponding to  $f_p \sim 10^{-1}$  Hz. The data have been scaled with the peak frequency  $f_p$  and peak amplitude  $\epsilon''_p$ , respectively. The upper right inset shows data for the heptamer, where the  $\alpha$  relaxation,  $\beta$  relaxation, and dc conductivity ( $\sigma$ ) are clearly seen. The lower left inset shows the derivatives of the data for  $T \sim T_g$ . The ordinate refers to the monomer data. The remaining data sets have been consecutively transposed with 0.25 for clarity. The data within the box is the derivative for the monomer at a temperature 11 K below  $T_g$ .

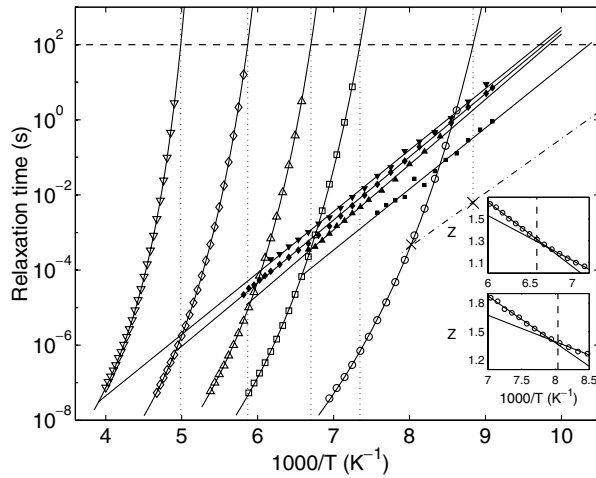


FIG. 2.  $\alpha$  and  $\beta$  relaxation times versus inverse temperature for the studied systems. The symbols are the same as in Fig. 1. The fits to the data are described in the text and are shown as solid lines. The dash-dotted line indicates  $\tau_\beta$  for the monomer as extrapolated from the other data sets. The uppermost inset shows  $Z$  versus  $1000/T$  for the dimer, and the lowermost for the monomer, where  $Z = [-d\log_{10}(f_p)/d(1/T)]^{-1/2} \times 100$  and  $f_p$  is the  $\alpha$  peak frequency. The vertical dashed lines in the insets mark  $1000/T_{\alpha\beta}$ , as obtained from the crossing of the  $\alpha$  relaxation and the extrapolated  $\beta$  relaxation.

including six different parameters plotted as a function of  $\log_{10}(M)$ . Figure 3(a) shows that the  $T_g$  values vary in a smooth fashion, which can be described approximately by a modified Fox-Flory relation (see figure caption). Figure 3(b) shows the temperatures  $T_g^\beta$ , i.e., the temperatures where the time scale of the  $\beta$  relaxations  $\tau_\beta$  reach 100 s. We note that the behavior of the  $T_g^\beta$  values drastically change for chains of less than a few units. A detailed discussion of the important length scales found in the analysis will be deferred to a subsequent publication [20]. Figure 3(c) shows the temperature  $T_{\alpha\beta}$ , where the  $\alpha$  and  $\beta$  relaxations would cross provided they are undisturbed by the presence of each other. Figure 3(d) shows the  $\beta$  relaxation time  $\tau_\beta$  for the various samples at three different temperatures  $T_i$  (see figure caption) within the measured range. Figure 3(e), in turn, depicts  $\tau_\beta(T_g)$ , and finally Fig. 3(f) shows the relaxation time  $\tau_{\alpha\beta}$  at the extrapolated crossing of the  $\alpha$  and  $\beta$  relaxation times.

The systematic nature of the  $M$  variation of all parameters suggests that it is indeed possible to reach quantitative information also about the location of the underlying  $\beta$  relaxation for the monomer. By the use of power law fits to the dimer, trimer, and heptamer data in Figs. 3(e) and 3(f) we can extrapolate to the monomer. The result gives two points located at  $[1000/T_g, \tau_\beta(T_g)]$  and  $[1000/T_{\alpha\beta}, \tau_{\alpha\beta}]$ , which are marked in Fig. 2 with crosses. An Arrhenius function that is consistent with these two data points results in the dash-dotted line shown in Fig. 2. Based on this function we calculate the resulting param-

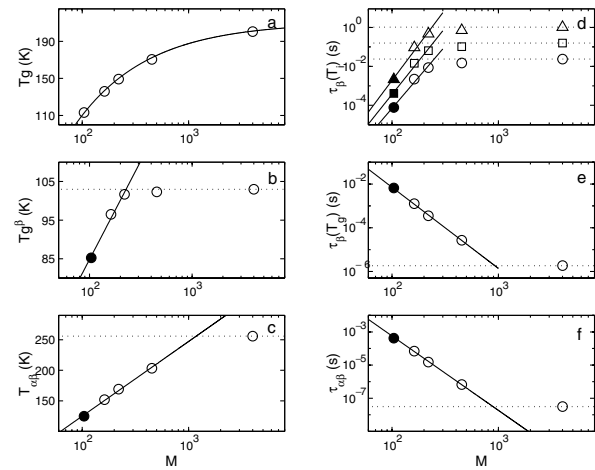


FIG. 3. Parameters, described in detail in the text, plotted vs  $M$  (unfilled symbols). The filled symbols indicate the values extrapolated for the monomer. The solid line in (a) is a fit to a modified Fox-Flory relation,  $T_g = T_g^\infty - A/M^\gamma$  with  $T_g^\infty = 211$  K,  $A = 1585$ , and  $\gamma = 0.6$ . (d) Data for  $1000/T_i = 7.5$  ( $\circ$ ),  $8$  ( $\square$ ), and  $8.5$  ( $\triangle$ ), respectively. The solid lines in (e) and (f) are power law fits to the data for the dimer, trimer, and heptamer. The solid lines in (b), (c), and (d) are guides to the eye. The dotted lines indicate the parameter values for the polymer. The errors in the displayed parameters are smaller than the size of the symbols.

ter values, which represent the monomer. The obtained results are shown as solid symbols in Fig. 3. We note that the temperature dependence of  $\tau_\beta$ , indicated by the dash-dotted line in Fig. 2, satisfies extrapolations to the monomer for all related characteristic properties Figs. 3(b)–3(f) very well. It should be emphasized that the  $\tau_\beta(T_i)$  and  $T_g^\beta$  are parameters solely referring to the secondary process, while  $\tau_{\alpha\beta}$ ,  $\tau_\beta(T_g)$ , and  $T_{\alpha\beta}$  combine information from both the  $\alpha$  and the  $\beta$  processes. We have thus found strong indications that the  $\beta$  relaxation of the monomer follows the Arrhenius temperature dependence shown by the dash-dotted line in Fig. 2. The activation energies are nearly identical throughout the series ( $\sim 0.32$ – $0.34$  eV), while  $\tau_\beta$  as well as  $\tau_\alpha$  varies systematically with  $M$ . The result is a gradual transformation from the strongly merged  $\alpha$  and  $\beta$  processes for the monomer (where the  $\beta$  process is observed only as an excess wing) to the well-separated  $\alpha$  and  $\beta$  loss peaks for the higher  $M$  samples.

Additional and independent evidence that the results of the analysis presented above is physically sound can be found in the two insets of Fig. 2. These are plots according to Stickel [25], in which data pertaining to a VFT relation show a linear behavior. For glass formers, it is well documented [25] that the VFT relation that describes the data at low temperatures, near  $T_g$ , will change into another VFT relation at some higher temperature,  $T_B$  [26]. It has been found that  $T_B$  signals changing dynamics in the material as observed in a whole range of different properties [27]. The most important observation for our

purposes is that to a good approximation one generally finds that  $T_{\alpha\beta} \approx T_B$ . The uppermost inset in Fig. 2 shows a Stickel plot for the dimer. We find as expected a crossover between two linear regimes. A glance at the main plot of Fig. 2 shows that this occurs very close to the extrapolated merging of the  $\alpha$  and  $\beta$  relaxations, also indicated by the vertical dashed line in the inset. The lowermost inset shows the corresponding plot for the monomer data. Again, a crossover between two linear regimes is found, which corresponds well with the location of the  $\alpha$ - $\beta$  merging, as predicted from our scaling analysis described above.

It has recently been argued that the excess wing is caused by an underlying  $\beta$  relaxation, but that this process has some features setting it aside from the J-G  $\beta$  relaxation (see, e.g., [12]). This conclusion was based on the temperature dependence of the  $\beta$  relaxation times,  $\tau_\beta$ , obtained from fitting the dielectric loss of a type A glass former with a sum of an asymmetric ( $\alpha$ ) and a symmetric ( $\beta$ ) loss shape. The result of such an analysis is that both relaxations follow each other closely in time. Two relaxations that are not well separated in time will merge [28], and a fitting routine not taking this into account will by necessity produce a secondary process following the primary one [29]. Based on our analysis, there is no evidence for a drastic change in the temperature dependence of the  $\beta$  relaxation constituting the excess wing. On the contrary, a simpler physical picture of an underlying  $\beta$  relaxation with a  $\tau_\beta$  following an Arrhenius dependence emerges. This implies that the excess wing, at least in this system, is due to an underlying  $\beta$  relaxation of the J-G type.

In conclusion, we have found direct evidence for a gradual transformation from widely separated to strongly merged  $\alpha$  and  $\beta$  relaxations in propylene glycol dimethyl ethers of varying chain length. Several characteristic temperatures and relaxation times display scaling relations with chain length. Taking advantage of this, it is possible to locate the  $\beta$  relaxation time for the monomer, even though the  $\beta$  process is hidden beneath the stronger  $\alpha$  peak. This  $\beta$  relaxation has the same characteristics as the  $\beta$  processes of the other members of this sample series. In general, this suggests that the main difference between type A and type B glass formers is the relaxation time at the merging temperature.

---

\*Electronic address: johanm@fy.chalmers.se

- [1] P.G. Debenedetti and F.H. Stillinger, *Nature* (London) **410**, 259 (2001).
- [2] G.P. Johari and M. Goldstein, *J. Chem. Phys.* **53**, 2372 (1970).
- [3] C. A. Angell, K. L. Ngai, G. B. McKenna, P. F. McMillan, and S. W. Martin, *J. Appl. Phys.* **88**, 3113 (2000).
- [4] K. L. Ngai, *J. Non-Cryst. Solids* **275**, 7 (2000).

- [5] G. Tarjus, D. Kivelson, and S. Kivelson, in *Supercooled Liquids, Advances and Novel Applications*, edited by J.T. Fourkas, D. Kivelson, U. Mohanty, and K.A. Nelson (American Chemical Society, Washington, DC, 1996).
- [6] R.V. Chamberlin, *Phys. Rev. Lett.* **82**, 2520 (1999).
- [7] C. León and K. L. Ngai, *J. Phys. Chem. B* **103**, 4045 (1999).
- [8] P. K. Dixon, L. Wu, S. R. Nagel, B. D. Williams, and J. P. Carini, *Phys. Rev. Lett.* **65**, 1108 (1990).
- [9] A. Kudlik, S. Benkhof, T. Blochowicz, C. Tschirwitz, and E. Rössler, *J. Mol. Struct.* **479**, 201 (1999).
- [10] N. B. Olsen, *J. Non-Cryst. Solids* **235–237**, 399 (1998).
- [11] U. Schneider, R. Brand, P. Lunkenheimer, and A. Loidl, *Phys. Rev. Lett.* **84**, 5560 (2000).
- [12] K. L. Ngai, P. Lunkenheimer, C. León, U. Schneider, R. Brand, and A. Loidl, *J. Chem. Phys.* **115**, 1405 (2001).
- [13] G. P. Johari and E. Whalley, *Faraday Symp. Chem. Soc.* **6**, 23 (1972).
- [14] M. Paluch, R. Casalini, S. Hensel-Bielowka, and C. M. Roland, *J. Chem. Phys.* **116**, 9839 (2002).
- [15] S. Hensel-Bielowka and M. Paluch, *Phys. Rev. Lett.* **89**, 025704 (2002).
- [16] C. León, K. L. Ngai, and C. M. Roland, *J. Chem. Phys.* **110**, 11 585 (1999).
- [17] A. Döss, M. Paluch, H. Sillescu, and G. Hinze, *Phys. Rev. Lett.* **88**, 095701 (2002).
- [18] R. Bergman, C. Svanberg, D. Andersson, A. Brodin, and L. M. Torell, *J. Non-Cryst. Solids* **235–237**, 225 (1998).
- [19] T. Alper, A. J. Bartow, and R.W. Grey, *Polymer* **17**, 665 (1976).
- [20] J. Mattsson, R. Bergman, P. Jacobsson, and L. Börjesson (to be published).
- [21] R. Bergman, *J. Appl. Phys.* **88**, 1356 (2000).
- [22] G. P. Johari, *Polymer* **27**, 866 (1986).
- [23] J. Wiedersich, T. Blochowicz, S. Benkhof, A. Kudlik, N.V. Surovtsev, C. Tschirwitz, V.N. Novikov, and E. Rössler, *J. Phys. Condens. Matter* **11**, A147 (1999).
- [24] Defined, e.g., as the slope of  $\log_{10}\tau_\alpha$  at  $T_g$  in an Arrhenius plot [3].
- [25] F. Stickel, E.W. Fischer, and R. Richert, *J. Chem. Phys.* **104**, 2043 (1996).
- [26] The data in Fig. 2 can be well described over a large dynamical range with a single VFT. What the derivative analysis demonstrates, however, is that a subtle change of the behavior occurs well within the experimental window for the lowest  $M$  samples.
- [27] A. P. Sokolov, *J. Non-Cryst. Solids* **235–237**, 190 (1998).
- [28] G. Williams, *Adv. Polym. Sci.* **33**, 60 (1979).
- [29] A straightforward explanation for the observed non-Arrhenius behavior is simply that a curve-fitting routine will position the  $\beta$  relaxation peak so that its high-frequency tail describes the wing while its low frequency tail affects the low frequency part of the  $\alpha$  peak as little as possible. The fit will thus place the  $\beta$  peak frequency somewhere between the  $\alpha$  peak maximum and the onset of the wing. The obtained  $\beta$  relaxation time will hence mimic the temperature dependence of the  $\alpha$  relaxation time.